A study of degenerate vibronic coupling effects on scattering processes: are resonances affected by degenerate vibronic coupling?

David M. Charutz [a], Roi Baer [b], Michael Baer [a]

[a] Department of Physics and Applied Mathematics, SOREQ NRC, Yavne 81800, Israel
[b] The Fritz Haber Institute for Molecular Dynamics, The Hebrew University, Jerusalem, Israel

Abstract

Recently the Jahn–Teller model was extended to treat (reactive) scattering processes. The present study is devoted to possible effects of a degenerate vibronic coupling (DVC) on resonances. The main conclusions are: (a) The DVC affects dramatically the state-to-state transition processes and as a result it shuffles resonances attached to given transitions and may cause existing resonances to be masked by other processes. (b) The DVC may affect the widths and the heights of resonances but change only slightly their position.

1. Introduction

The possible effects of degenerate vibronic coupling (DVC), as for instance conical intersections (CI), on scattering processes have become an important subject within the study of few-atom systems [1–7]. In that light we developed a two-coordinate model which is close in spirit to the Jahn–Teller (JT) model [8–19] but is devised for studying the effects of CIs and eventual other similar degenerate electronic situations on scattering processes [17]. The main motivation for doing that is to have a model which is simple enough to be solved to any required accuracy but still general so that calculated magnitudes such as S-matrix elements and transition probabilities bear a relation to realistic systems. In our first publication on this subject [17] we were mainly interested in verifying that the ordinary Born–Oppenheimer approximation (BOA) [20] fails even for energies much below the upper surface (similar effects of DVCs on molecular spectra have been known for some time [13]). In order to stay within the spirit of the BOA a new equation was presented [17,19]. In a detailed numerical study it was shown that results due to this equation and results obtained by solving the two coupled equations (namely, solving the model without approximations) are similar and that both differ significantly from results due to the BOA.

In the present publication we concentrate on (reactive) resonances and employing the simple two-coordinate model we show relevant results. Although simple, the model produces resonances and the main purpose of the present Letter is to study the effect of DVC on resonances.

This Letter is organized in the following way: the next section gives some theoretical remarks relevant to the subject under consideration, the third section presents the quasi-JT (scattering) model, the fourth

shows and discusses numerical results, and the fifth summarizes the conclusions.

2. Theoretical remarks

A detailed derivation of the Schrödinger equations that must be solved was given in our previous publication [17]. Here are presented the relevant equations accompanied by short explanations.

The two coupled equations that have to be solved to obtain the accurate results are [17–19]:

$$\left[T_n + \bar{u}_1 - E\right]\chi_1 + \frac{1}{2mq^2}\frac{\partial}{\partial\varphi}\chi_2 = 0,$$

$$\left[T_n + \bar{u}_2 - E\right]\chi_2 - \frac{1}{2mq^2}\frac{\partial}{\partial\varphi}\chi_1 = 0, \qquad (1)$$

where T_n is the kinetic operator given in the form

$$T_n = -\frac{1}{2m}\left[\frac{\partial^2}{\partial q^2} + \frac{1}{q}\frac{\partial}{\partial q} + \frac{1}{q^2}\frac{\partial^2}{\partial\varphi^2}\right], \qquad (2)$$

q and φ are two polar coordinates, m is the mass of the system, E is the total energy of the system and $\bar{u}_i$; $i = 1, 2$ are defined as:

$$\bar{u}_i = u_i + \frac{1}{8mq^2}; \quad i = 1, 2. \qquad (3)$$

Here, u_i; $i = 1, 2$ are the two adiabatic potential energy surfaces (PES).

Eqs. (1) can be solved directly but we preferred to do so by transforming them to the diabatic representation. This is done by employing the following adiabatic–diabatic transformation [18,21–24]:

$$\begin{pmatrix} \chi_1 \\ \chi_2 \end{pmatrix} = \begin{pmatrix} \cos\alpha & -\sin\alpha \\ \sin\alpha & \cos\alpha \end{pmatrix}\begin{pmatrix} \eta_1 \\ \eta_2 \end{pmatrix}. \qquad (4)$$

Substituting Eq. (4) in Eq. (1) it can be shown [18,21–24] that choosing α to be

$$\alpha = \tfrac{1}{2}\varphi \qquad (5)$$

annihilates the coefficients of the first derivatives and leads to the following (diabatic) equations:

$$\left\{T_n + \tfrac{1}{2}\left[u_1 + u_2 + (u_1 - u_2)\cos\varphi\right]\right\}\eta_1$$

$$- \tfrac{1}{2}(u_1 - u_2)\sin\varphi\eta_2 = E\eta_1,$$

$$\left\{T_n + \tfrac{1}{2}\left[u_1 + u_2 - (u_1 - u_2)\cos\varphi\right]\right\}\eta_2$$

$$- \tfrac{1}{2}(u_1 - u_2)\sin\varphi\eta_1 = E\eta_2. \qquad (6)$$

The results obtained from this coupled-equation model will be compared with those obtained by the ordinary (single surface) Born–Oppenheimer model, namely:

$$(T_n + u - E)\chi = 0, \qquad (7)$$

where u_1 and χ_1 are replaced by u and χ, respectively.

The two-coupled equations in Eq. (6) and the single equation in Eq. (7) are solved using a recent method based on combining the discrete-variable representation with the features of the Toeplitz matrix [25–28].

3. The model system

The model system is reminiscent of the Teller model [9] which is the original model for representing a conical intersection (CI). Within the Teller model are considered two *diabatic* potential energy surfaces (PES) which intersect at a point and which are, at this point's vicinity, linearly dependent on the coordinates. The model, as a whole, is used to treat bound systems. Our model is devised to treat scattering processes and therefore is assumed to be bound with respect to one (Cartesian) coordinate, i.e. r and unbound with respect to the other coordinate, i.e. R. Since we are interested in simulating a reactive process the model potential will possess two asymptotes; one at $R \approx \infty$ and the other at $R \approx -\infty$. In addition, mainly for reasons of clarity (as will be discussed in the next section), the dependence of the *adiabatic* potentials on R and r, in the vicinity of the intersection point between the two surfaces, is not linear but quadratic. This change makes the present model typical for a wider range of couplings,

Table 1
List of parameters applied in the calculations

all models:	
m	0.58 proton mass
A	3.0 eV
D	5.0 eV
σ	0.30 Å
σ_1	0.75 Å
ω_0	39.14 10^{13} s^{-1}
ω_1	7.83 10^{13} s^{-1}
RSSM only:	
c	1.8 eV
d	8.0 eV
l	0.135 Å
NRDSM only:	
ρ	0.333 Å
R_f	-2.403 Å

namely the degenerate vibronic coupling (DVC). These changes are not expected to affect the physical content of the model because they are not directly associated with symmetry effects caused by the diabatic intersection. The symmetry effects enter through the *non-adiabatic* coupling term $\tau_\varphi(q, \varphi)$ which is the coefficient of the (first) φ derivative term in the *adiabatic* representation [19]. For the present model

it was shown in Ref. [17] that $\tau_\varphi(q, \varphi)$ is equal to $(2q)^{-1}$. A similar derivation with exactly the same expression for $\tau_\varphi(q, \varphi)$ was derived by Baer and Englman for the ordinary JT model (with a CI) [18]. Since $\tau_\varphi(q, \varphi)$ is the only term to determine the symmetry effects and since it is the same in the two models, the *symmetry* effects encountered in the two models have to be the same and are independent of the exact forms of the two adiabatic PESs. They may be linear in the vicinity of the intersection (and then the model is the ordinary JT model) or they may exhibit any other kind of dependence (in our present model they are quadratic) but this, as we just proved, will not affect the symmetry.

The two *adiabatic* PESs u_1 and u_2 are assumed to be, in this study, of the forms

$$u_1(R, r) = \tfrac{1}{2}m\big(\omega_0 - \tilde{\omega}_1(R)\big)^2 r^2 + Af(R, r),$$
(8a)

$$u_2(R, r) = \tfrac{1}{2}m\omega_0^2 r^2 - (D - A)f(R, r) + D,$$
(8b)

where A, D and ω_0 are constants. The function $f(R, r)$, which is responsible for forming a single
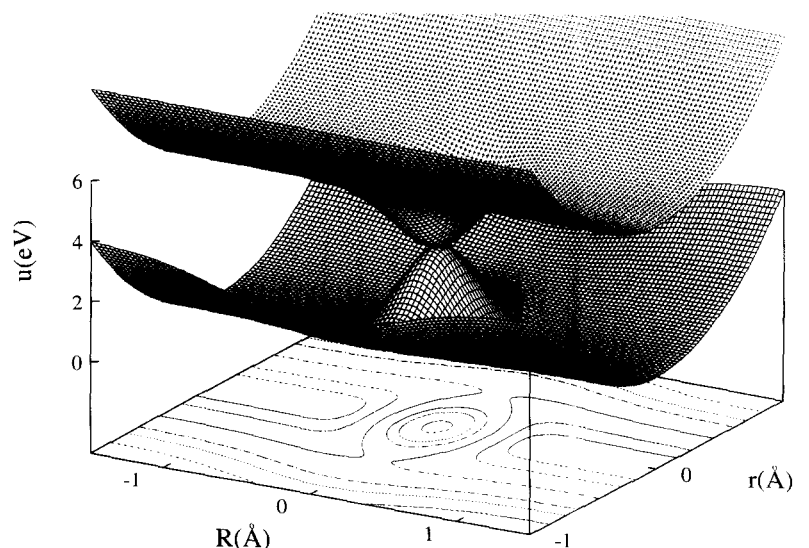

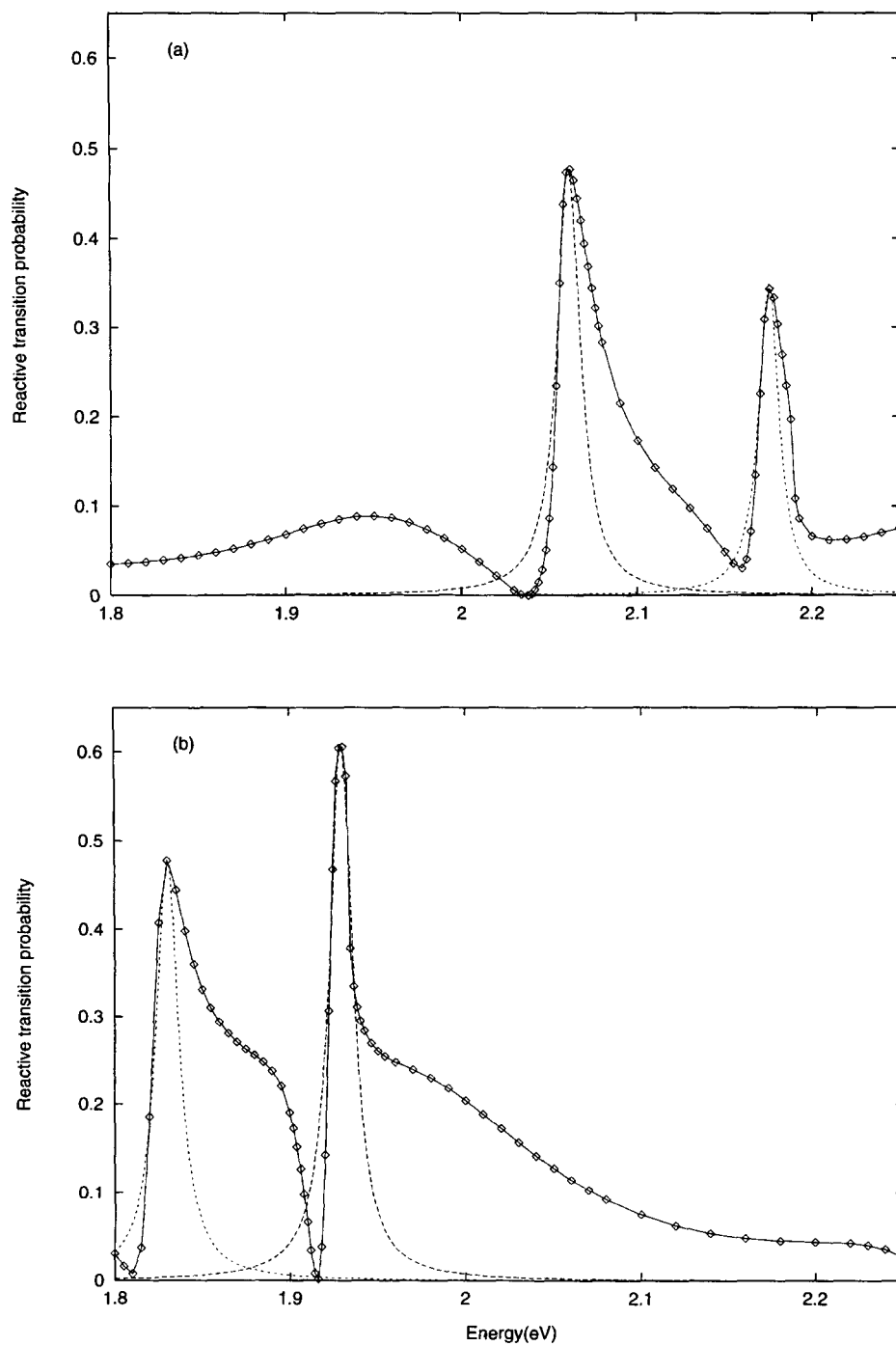Fig. 1. The two adiabatic potential energy surfaces applied in the extended Jahn–Teller model.

Fig. 2. Reactive transition probability as a function of total energy, calculated within the Born Oppenheimer approximation: (a) Results for the 0 → 0 transition; (b) results for the 1 → 1 transition; (————) quantum mechanical results; (– – –) Lorentzian fitted curves.

intersection point between the two PESs, is assumed to be

$$f(R, r) = \exp\left(-\frac{R^2 + r^2}{\sigma^2}\right), \tag{9}$$

and $\tilde{\omega}_1(R)$, which is responsible for forming a bifurcated transition state, is assumed to be

$$\tilde{\omega}_1(R) = \omega_1 \exp\left(-(R/\sigma_1)^2\right). \tag{10}$$

Here σ, σ_1 and ω_1 are constants, r is the vibrational coordinate and R is the translational coordinate (both are defined along the interval $-\infty \leqslant x \leqslant +\infty$; $x = r$, R). The numerical values of the various parameters are listed in Table 1. They were chosen to be relevant for a typical chemical reaction; the mass is assumed to the reduced mass of $H + H_2$ and the vibronic spacing is about 0.25 eV. The two adiabatic PESs are presented in Fig. 1.

4. Results

We shall examine the effects of the DVC on resonances and for this purpose we consider the energy range 1.8–2.25 eV. It is important to remember that this energy range is below the intersection energy point ($= 3$ eV).

In Fig. 2 are presented the (reactive) probabilities $P(0, 0)$ and $P(1, 1)$ as a function of total energy. The results were obtained by solving Eq. (7), namely, the ordinary BO Schrödinger equation. It is important to emphasize that the PESs employed in this study are even with respect to the vibrational coordinate r and therefore only (even $\to$ even) and (odd $\to$ odd) transitions are allowed. Thus the probabilities $P(0, 1)$ and $P(1, 0)$ are identically zero. As can be seen, both the $P(0, 0)$ and $P(1, 1)$ curves are characterized by two well-separated resonances, each of

which is located at a different energy. To find the characteristic features of the resonances they were fitted to Lorentzians so that their heights, A, their half width, Γ, and their positions E_0, were determined by 'trial and error'. The positions, widths and heights of the various fitted Lorentzians are given in Table 2 and the fits are drawn as dashed lines in Fig. 2 (and also in Fig. 4). It is important to mention that all other probability functions, namely the even ones $P(0, v')$ and the odd ones $P(1, v')$ have resonances at the same energies as $P(0, 0)$ and $P(1, 1)$, respectively. In all cases the resonances can be identified as Feshbach-type resonances [29] for which the position of the resonance coincides with an eigenvalue, $\tilde{\varepsilon}$, of a vibrational potential curve $\varepsilon(R)$ [29,30]. These vibrational potential curves are usually calculated by solving the following R-dependent eigenvalue problem:

$$\left(-\frac{1}{2m}\frac{\partial^2}{\partial r^2} + u_1(r \mid R) - \varepsilon_n(R)\right)\zeta_n(r \mid R) = 0, \tag{12}$$

where $u_1(r \mid R) \equiv u_1(r, R)$ is the lower adiabatic PES and r and R are equal to $q \sin \varphi$ and $q \cos \varphi$, respectively.

In our present model the resonances associated with the even probability functions $P(0, v')$ are identified with eigenvalues of the even adiabatic vibrational curves and the resonances associated with odd probability functions $P(1, v')$ are identified with the odd vibrational curves. Following an inspection of the vibrational potential curves $\varepsilon_n(R)$ obtained from Eq. (12) we found that the positions of the resonances of the $P(0, 0)$ and $P(1, 1)$ probability functions are associated with the $\varepsilon_8(R)$ and $\varepsilon_7(R)$ curves, respectively (see Fig. 3). In addition to the curves, the corresponding eigenvalues $\tilde{\varepsilon}_{8,i}$; $i = 1, 2$ and $\tilde{\varepsilon}_{7,i}$; $i = 1, 2$ are listed in Table 2.

Table 2
Lorentzian parameters and eigenvalues related to BOA resonances (in eV)

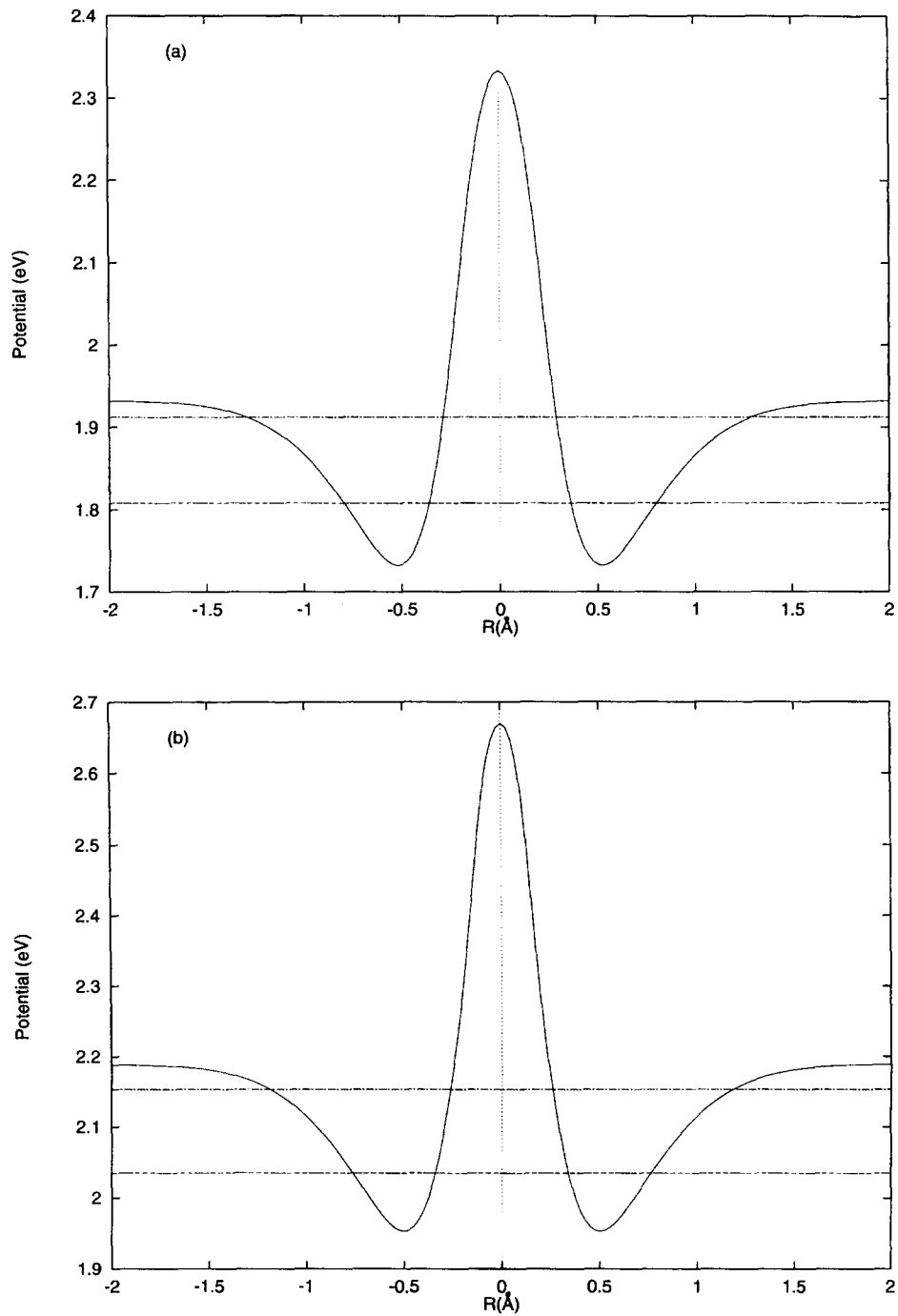| Transition	A	Γ	E_0	$\tilde{\varepsilon}$
$0 \to 0$	0.480	0.016	2.06	2.03
$0 \to 0$	0.350	0.014	2.18	2.15
$1 \to 1$	0.478	0.016	1.83	1.81
$1 \to 1$	0.610	0.016	1.93	1.91

Fig. 3. Vibrational adiabatic curves as a function of R. Also shown are the position of the eigenvalues. (a) The 8th curve; (b) the 9th curve.
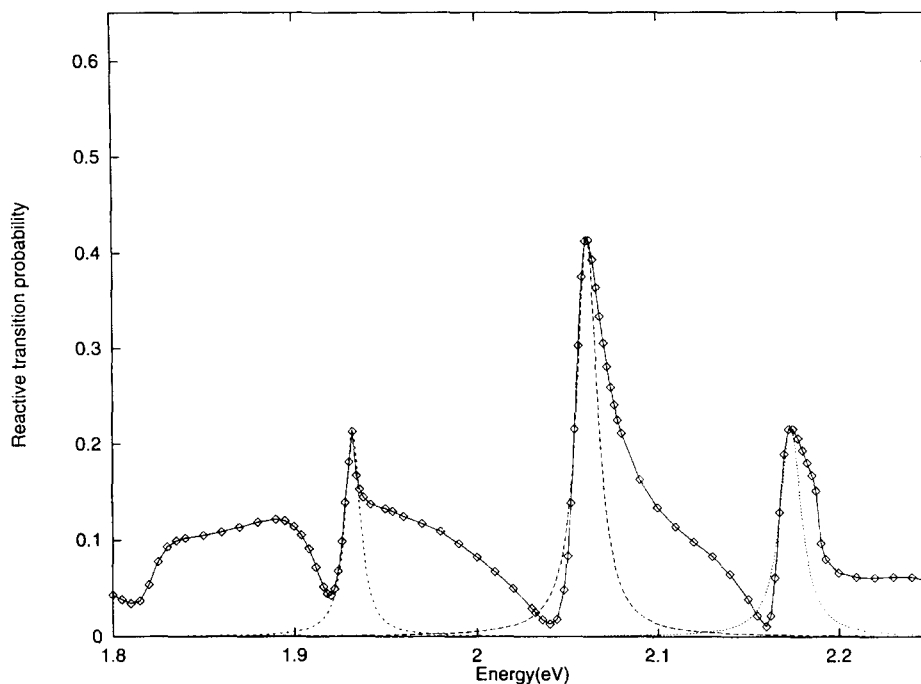
Fig. 4. Conical intersection-affected reactive transition probability $P(0 \leftrightarrow 1)$ as a function of total energy. (———) Quantum mechanical results; (- - -) Lorentzian fitted curves.

Fig. 4 shows the transition probabilities $P(0, 1)$ as a function of energy derived from the solutions of the set of coupled equations in Eq. (6). As before, the resonances were analyzed by fitting them to Lorentzians; their positions, widths and heights are in Table 3.

Two important differences are noticed between the BOA and the coupled-equations results:

(a) In contrast to the BOA results we find here that

$$P(\text{even} \rightarrow \text{even}) = P(\text{odd} \rightarrow \text{odd}) = 0,$$

but then

$$P(\text{even} \leftrightarrow \text{odd}) \neq 0.$$

(b) The transition probability curves contain four resonances, instead of two as in each of the previous cases. We included also the unidentified shape in the energy interval 1.8–1.9 eV because it seems that there is a resonance which is masked by other effects.

The effect of the DVC is indeed dramatic: it changes the character of the transition (namely, it causes it to be odd $\leftrightarrow$ even) and it changes entirely the pattern of the resonances. Whereas the first subject was elaborated in Ref. [17], here we concentrate on the second subject, namely on the effect of the DVC on resonances. The DVC not only caused the two 'even' and the two 'odd' resonances to

Table 3
Lorentzian parameters and eigenvalues related to conical intersection effected resonances (in eV)

Transition	A	Γ	E_0	$\tilde{\varepsilon}$	$\tilde{\varepsilon}_c$
$0 \rightarrow 1$	0.215	0.010	1.93	1.91	1.92
$0 \rightarrow 1$	0.420	0.014	2.06	2.03	2.04
$0 \rightarrow 1$	0.220	0.014	2.17	2.15	2.23

manifest themselves through a single even–odd transition, but it also affected the overall shape of each of the resonances; it caused one resonance to be masked by unresolved processes and it varied some characteristic parameters related to the other three, namely, the heights, A, which are reduced and the half widths, Γ, which are narrowed (see Tables 2 and 3 for comparison). The only feature which was hardly affected was their position, E_0, and the reason is as follows.

The DVC-affected results were obtained by solving the two coupled equations in Eq. (6). In Ref. [17] we showed that the low-energy transition probabilities due to the coupled equations in Eq. (6) and those derived by employing an extended BOA single-surface equation of the form (Eq. (13') in Ref. [17])

$$\left(T_n + \bar{u} + \frac{i}{2mq^2}\frac{\partial}{\partial\varphi} - E\right)\tilde{\chi} = 0 \qquad (13)$$

are, for all practical purposes, identical. In other words, the transition probability functions, including the resonances formed by solving Eq. (6), were reproduced by solving Eq. (13). Although written in terms of polar coordinates, Eq. (13) was solved using the Cartesian coordinates (r, R).

As mentioned above, the positions of the resonances are solely determined by the eigenvalues of the adiabatic curves. Therefore we have to calculate adiabatic curves employing an equation that follows from Eq. (13). Due to the angular symmetry introduced by the DVC it will be more convenient to use, for this purpose, polar coordinates, namely (q, φ); thus φ will be the internal coordinate and q will serve as a parameter. Therefore the relevant q-dependent equation to determine the internal adiabatic potential curves $\varepsilon_{c_n}(q)$ is

$$\left\{-\frac{1}{2mq^2}\frac{\partial^2}{\partial\varphi^2} + u_1(\varphi\,|\,q) + \frac{1}{8mq^2}\right.$$

$$\left.-\frac{i}{2mq^2}\frac{\partial}{\partial\varphi} - \varepsilon_{c_n}(q)\right\}\xi_n(\varphi\,|\,q) = 0. \qquad (14)$$

Eq. (14) yields rotational (instead of vibrational) adiabatic curves. As before the adiabatic curves can support q-dependent bound states which are responsible for the Feshbach resonances. It is important to mention that the q-dependent eigenvalues are essen-

tially the same as those that were obtained ignoring the terms due to the DVC (the third and the fourth terms in Eq. (14)) but the eigenfunctions were different because they are anti-symmetric with respect to φ and therefore flip sign at $\varphi = 2\pi$. Having the q-dependent potential curves we calculated the corresponding eigenvalues which are also listed in Table 3. The results for $\tilde{\varepsilon}_n$ and $\tilde{\varepsilon}_{c_n}$ are similar, thus justifying the expectations that the resonances within the two frameworks are the same.

5. Conclusions

The main conclusions are as follows:

(a) The DVC affects dramatically the state-to-state transition processes and as a result resonances attached to given transitions undergo shuffling. Moreover it causes existing resonances to disappear or at least to be significantly weakened by other processes.

(b) The DVC affects the width and the height of resonances but only slightly their position.

It is not yet clear to what extent DVC will affect scattering processes in realistic systems but resonances (or differential cross sections) must be analyzed with care when DVC effects are expected. The situation in case of spectroscopic measurements may be more delicate because here the analysis is done separately for each value of the total angular momentum J and in such cases the effect of resonances will be more pronounced as compared to the case with scattering processes where it is averaged over many J values.

References

[1] B. Lepetit and A. Kuppermann, Chem. Phys. Lett. 166 (1990) 581.
[2] Y.-S.M. Wu, A. Kuppermann and B. Lepetit, Chem. Phys. Lett. 186 (1991) 319.
[3] A. Kuppermann and Y.-S.M. Wu, Chem. Phys. Lett. 205 (1993) 577.
[4] Y.-S.M. Wu and A. Kuppermann, Chem. Phys. Lett. 235 (1995) 105.
[5] A. Kuppermann and Y.-S.M. Wu, Chem. Phys. Lett. 241 (1995) 229.
[6] X. Wu, R.E. Wyatt and M. D'mello, J. Chem. Phys. 101 (1994) 2953.

[7] N. Markovic and G.D. Billing, J. Chem. Phys. 100 (1994) 1089.

[8] R. Englman, The Jahn-Teller effect in molecules and crystals (Wiley-Interscience, New York, 1972).

[9] E. Teller, J. Phys. Chem. 41 (1937) 109.

[10] H.C. Longuet-Higgins, U. Opik, M.H.L. Pryce and R.A. Sack, Proc. R. Soc. London Ser. A 244 (1958) 1.

[11] M.S. Child and H.C. Longuet-Higgins, Phil. Trans. R. Soc. London Ser. A 254 (1961) 259.

[12] G. Herzberg and H.C. Longuet-Higgins, Discuss. Faraday Soc. 35 (1963) 77.

[13] H. Koppel, W. Domcke and L.S. Cederbaum, Adv. Chem. Phys. 57 (1984) 59.

[14] D.G. Truhlar and C.A. Mead, J. Chem. Phys. 77 (1982) 6090.

[15] W. Duch and G.A. Segal J. Chem. Phys. 79 (1983) 2951; 82 (1985) 2392.

[16] J. Schon and H. Koppel, J. Chem. Phys. 103 (1995) 9292.

[17] R. Baer, D.M. Charutz, R. Kosloff and M. Baer, J. Chem. Phys. 105 (1996) 9141.

[18] M. Baer and R. Englmann, Mol. Phys. 75 (1992) 293.

[19] M. Baer and R. Englmann, Chem. Phys. Lett., in press.

[20] M. Born and J.R. Oppenheimer, Ann. Phys. (Leipzig) 84 (1927) 457.

[21] M. Baer, Chem. Phys. Lett. 35 (1975) 112.

[22] Z.H. Top and M. Baer, J. Chem. Phys. 66 (1977) 1363; Chem. Phys. 25 (1977) 1.

[23] M. Baer, Mol. Phys. 40 (1980) 1011.

[24] T. Pacher, L.S. Cederbaum and H. Koppel, Adv. Chem. Phys. 84 (1993) 293.

[25] M. Gilibert, A. Baram, H. Szichman and M. Baer, J. Chem. Phys. 99 (1993) 3503.

[26] E. Eisenberg, S. Ron and M. Baer, J. Chem. Phys. 101 (1994) 3802.

[27] D.M. Charutz, S. Ron, E. Eisenberg and M. Baer, Chem. Phys. Lett. 244 (1995) 299.

[28] E. Eisenberg, D.M. Charutz, S. Ron and M. Baer, J. Chem. Phys. 104 (1996) 1886.

[29] H. Feshbach, Ann. Phys. 5 (1958) 357.

[30] M. Baer, in: The theory of chemical reaction dynamics, Vol. I. ed. M. Baer (CRC Press, Boca Raton, FL, 1985) chap. 3.